J Mol Model (2012) 18:4547–4556
DOI 10.1007/s00894-012-1461-9

ORIGINAL PAPER

Selectivity of labeled bromoethylamine for protein alkylation

Simona Marincean · Montserrat Rabago Smith · Laci Beltz · Babak Borhan

Received: 10 March 2012 / Accepted: 4 May 2012 / Published online: 29 May 2012
© Springer-Verlag 2012

Abstract Alkylation of cysteine residues has been used extensively for characterization of proteins and their mode of action in biological systems, research endeavors that are at the core of proteomics. Treatment with a simple alkylating agent such as [2-^{13}C] bromoethylamine would result in labeled thialysine at the ε-position. This chemical modification of proteins would allow investigations via both ^{13}C NMR spectroscopy and mass spectrometry. However [2-^{13}C] labeled bromoethylamine is not available commercially. We investigated its synthesis at acid pH with the goal of obtaining singly labeled bromoethylamine and understanding the mechanistic details of the reaction. Based on our experimental and theoretical results, bromination of [2-^{13}C] labeled ethanolamine in acidic conditions takes place via exclusive attack of the nucleophile (HBr) at the hydroxyl bearing C. Moreover, hydrogen bonding guides the nucleophilic attack, resulting in no label scrambling of the bromoethylamine product. Protein alkylation at cysteine residue with the synthesized $Br^{13}CH_2CH_2NH_2$-HBr is successful. Ab initio calculations in which CH_3SH serves as a model for the cysteine residue suggest that in gas phase intermolecular attack by the sulfur bearing nucleophile is favored over the intramolecular substitution by the amino group by 15.4 kJ mol^{-1}. Solution modeling shows that the trend is preserved at basic pH, which is the experimental one, but is reversed at neutral pH.

Keywords 13C label · Nucleophilic substitution · Bromoethylamine · Proteomics · Ab initio · Thiol

Electronic supplementary material The online version of this article (doi:10.1007/s00894-012-1461-9) contains supplementary material, which is available to authorized users.

S. Marincean (✉)
Department of Natural Sciences, University of Michigan-Dearborn,
4901 Evergreen Rd.,
Dearborn, MI 48128, USA
e-mail: simonam@umd.umich.edu

M. Rabago Smith · L. Beltz
Department of Chemistry and Biochemistry,
Kettering University,
1700 University Ave,
Flint, MI 48504, USA

B. Borhan
Department of Chemistry, Michigan State University,
East Lansing, MI 48824, USA

Introduction

Proteomics, an important emerging field, concerns mainly the protein profiling of complex biological samples, identification of affected proteins and study of protein–protein interactions and functions [1, 2]. Characterization of proteins as well as mechanistic studies are performed via techniques such as in-gel derivatization and site specific amino acid replacement [3, 4]. According to Hermanson [5], cysteine residues are the amino acids most frequently used for alkylation or "tagging" due to their specificity towards nucleophilic substitution [6]. Cysteine was ranked the most nucleophilic amino acid on the nucleophilicity scale created by Brotzel and Mayr [7]. The most common alkylating agents are ethylenimine, iodoacetate, 2-bromoethylamine, acrylamide, maleimide and (iodoethyl)trifluoroacetamide [7–13]. In all the above-mentioned alkylations (except iodoacetate), the product resembles a lysine residue, Fig. 1, in which a methylene (1) is replaced by a sulfur (2). Formation of γ-thiolysine (2), via alkylation of cysteine, has been reported to lead to recovery of the protein activity and formation of extra tryptic cut sites [14]. The modified cysteines are used in MS-proteomics, isotopic labeling, and chemical modification rescue [15, 16]. Of the above-

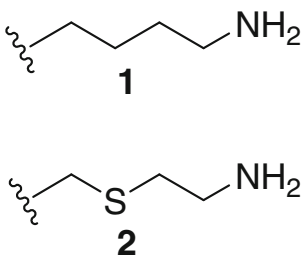

Fig. 1 Structure of lysine (1) and thiolysine (2)

mentioned alkylating agents, the only ones that can be used in chemical modification rescue right after alkylation are BEA and ethylenimine. It has been reported recently that use of BEA as alkylating agent requires careful control of the pH—a precaution that is not necessary for the more toxic ethylenimine [17]. The commercially available bromoethylamine and its fully deuterated equivalent has been used widely in MS-proteomics [13], isotopic labeling and chemical modification rescue [18, 19]. Treatment of proteins with labeled 2-bromoethylamine would result in ^{13}C labeled thiolysine (Scheme 1) at the ε-position. While this specific alkylating agent, 2-bromoethylamine seems attractive due to its simplicity, and its synthesis from ethanolamine in basic conditions has been reported previously [20–23], ^{13}C labeled bromoethylamine is not available commercially. Moreover, there is no complete agreement over the reaction mechanism in basic conditions. Two different pathways have been proposed, with the major difference being the presence of aziridine as an intermediate (Scheme 2a) [24]. The existence of aziridine would lead to a scrambled product if one starts with a ^{13}C labeled ethanolamine. However, in acidic conditions (Scheme 2b) the formation of aziridine ring should be precluded as the amino group would be protonated and therefore unable to displace the hydroxyl group in nucleophilic manner. At the same time, protonation of the amino group would enable both protonated amino and hydroxyl groups to act as leaving groups, hydroxyl being favored.

Protein alkylation at the cysteine residue using bromoethylamine takes place at a slightly basic pH and two reactions can be envisioned (Scheme 3). If the amino group acts as a nucleophile, an intramolecular nucleophilic substitution might occur first, leading to scrambling (Scheme 3a). This pathway also raises the question of the aziridinium ring existence as an intermediate. On the other hand if the thiol group from cysteine residue is the attacking nucleophile via an intermolecular attack (Scheme 3b), the label will be preserved at the initial C from bromoethylamine.

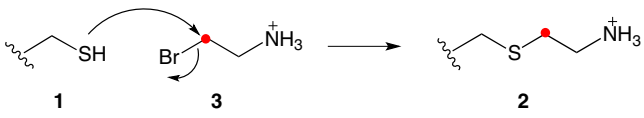

Scheme 1 Alkylation of cysteine with bromoethylamine

This report discusses the experimental and theoretical results of bromination of labeled ethanolamine in acidic conditions: no scrambling was observed due presumably to selective attack of the nucleophile (HBr) at the C bearing the OH functional group. Additionally, an example alkylation of proteins using $Br^{13}CH_2CH_2NH_2$-HBr is provided showing that the reaction is successful. Computational investigation of the alkylation reaction of bromoethylamine using a model system showed that aziridine ring formation is disfavored compared with direct attack of thiol group in gas phase and at basic pH in solution.

Methods

Experimental

Labeled ethanolamine was purchased from Cambridge Isotope Laboratories (Andover, MA) (2-^{13}C, 99 % $HO^{13}CH_2CH_2NH_2$-HCl). The hydrobromic acid (40 %) was obtained from Fisher Scientific (http://www.fishersci.com). The synthesis of labeled ethanolamine was accomplished by addition of HBr (2 eq., 0.072 mmol) dropwise to the labeled $HO^{13}CH_2CH_2NH_2$-HCl (5 mg, 0.036 mmol) and refluxing overnight. In vacuo solvent removal provided the bromoethylamine salt in an 87 % yield.

To evaluate the application potential of bromoethylamine as an alkylating agent, a cellular retinoic acid binding protein II R132K:R111L:L121E (CRABPII-KLE) protein that binds to all trans-retinal as a protonated Schiff base through a lysine at position 132 was mutated to a cysteine residue CRABPII-C132K:R111L:L121E (CRABPII-CLE). Site-directed mutagenesis was performed using the CRABPII-pET17b plasmid following Stratagene's Quikchange Kit protocol. The primers used for the mutation were: 5′-GACGTTGTGTGCACCTGCGTCTACGTCCGAGAG-3′ and 5′- CTCTCGGACGTAGACGCAGGTGCACACAAC GTC- 3′: The expression of the CRABPII proteins was carried out as previously described. The protein was isolated and purified using previously reported protocols [25]. Alkylation of the protein was accomplished by adding 100 equivalents of bromoethylamine to 1.5 mL of a 0.5 mg/mL protein solution (pH 8.5) at 50 °C for 6 h. The solution was then concentrated using mini filters, followed by a buffer exchange to pH 7.5 (phosphate buffer). The formation of a retinal-protonated Schiff base (PSB) was monitored via UV–VIS spectroscopy using a Cary300 BioWinUV spectrophotometer (Varian).

Scheme 2 Reaction pathways for bromination of ethanolamine

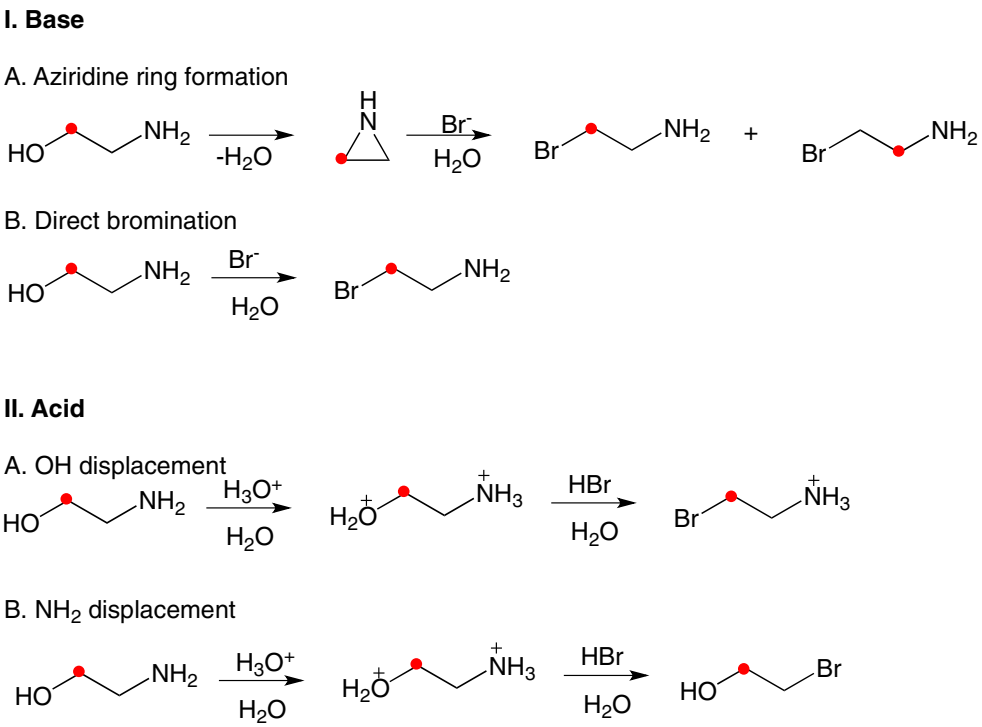

Computational

All calculations were done with the GAUSSIAN 09 program package [26]. The geometry optimizations were carried out with second order Møller-Plesset theory, MP2, [27] as well as with B3LYP [28–30] and OLYP [31] density functionals in conjunction with the 6-311++G** basis set [32–35].

DFT methods are popular choices over more expensive methods such as MP2; B3LYP and OLYP have been reported to give satisfactory results [36–43] in agreement with those obtained with highly correlated methods, with OLYP performing slightly better [40] than B3LYP. However, there has been concern over underestimation of the energetics, both activation barrier and overall reaction energy in reactions [44–48]. In order to alleviate such concerns, computations were performed at levels of theory mentioned above and the results compared. The trends were found to be similar regardless of the theory level, and the results are summarized in Tables 1 and 2. We will discuss henceforth only results obtained at MP2 level but the energetic profiles obtained with the DFT methods are provided in the supplemental information.

Scheme 3 Reaction pathways for alkylation of bromoethylamine

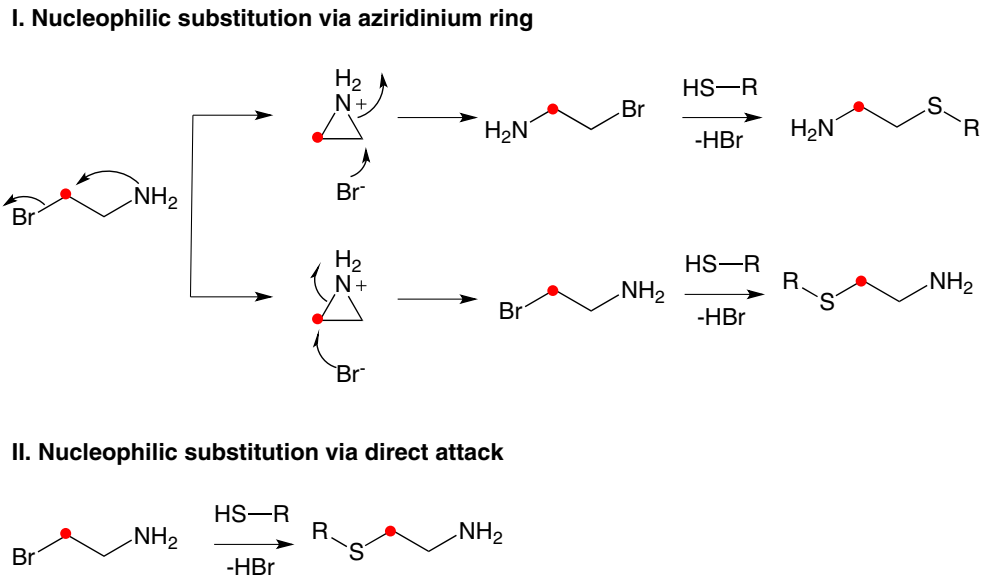

Table 1 Activation barrier for bromination of ethanolamine

Starting complex	Product	Theory	Activation barrier[a, b]
$HBr…NH_3CH_2CH_2OH_2$	$NH_3CH_2CH_2Br$	MP2	80.3 (109.6)
		B3LYP	55.0 (86.3)
		OLYP	53.7 (94.5)
$HBr…OH_2CH_2CH_2NH_3$	$OH_2CH_2CH_2Br$	MP2	247.7 (264.4)
		B3LYP	216.8 (234.0)
		OLYP	214.4 (232.3)

[a]Energies are corrected with ZPVE and expressed in kJ mol^{-1}

[b]First values are for gas-phase calculations, while values in parenthesis correspond to the solution reactions, at MP2/6-311 ++G**

The solvent, water, was incorporated in calculations as a continuum medium characterized by a dielectric constant via the CPCM model [49, 50]. Stationary points on the potential energy surfaces were characterized by vibrational analysis as minima or transition structures, having zero and one imaginary frequency, respectively. Intrinsic reaction coordinate (IRC) calculations were performed to confirm that reaction paths from transition structures relaxed to the expected ground states. The computed activation barriers were corrected for zero point vibrational energies. Structures were visualized using CYLview [51].

Results and discussion

Synthesis of $Br^{13}CH_2CH_2NH_2$-HBr

$Br^{13}CH_2CH_2NH_2$-HBr was prepared by refluxing two equivalents of HBr with $HO^{13}CH_2CH_2NH_2$-HCl overnight. ^{13}C NMR spectra of the isolated product showed, while there was a small amount of unreacted material as evidenced by a peak around 58 ppm belonging to the ^{13}C-OH, the only other peak was detected at 29.0 ppm corresponding to the ^{13}C-Br, Fig. 2, suggesting no label (^{13}C) scrambling. This finding is augmented by the absence of the peaks in the region belonging to ^{13}C-NH_3, around 42 ppm. Moreover in the corresponding ^1H NMR spectrum the splitting pattern for the $^{13}CH_2$ signal shows a coupling constant for ^{13}C–H of J=150.5 Hz, a value that is in the expected range. This data suggests that the mechanism for the bromination occurs via an intermolecular reaction, with selective attack at the OH site, and no aziridium intermediate (Scheme 2b).

Table 2 Activation barrier for alkylation of bromoethylamine

Nucleophile	Theory	Activation barrier[a, b]
CH_3SH	MP2	186.6 (128.4)
	B3LYP	151.3 (88.5)
	OLYP	148.0 (93.4)
CH_3S^-	MP2	33.9 (64.9)
	B3LYP	7.9 (36.8)
	OLYP	22.1 (48.9)
NH_2	MP2	198.3 (105.0)
	B3LYP	178.0 (73.0)
	OLYP	174.4 (70.3)

[a] Energies are corrected with ZPVE and expressed in kJ mol^{-1}

[b] First values are for gas-phase calculations, while values in parenthesis correspond to the solution reactions, at MP2/6-311++G**

Protein alkylation with $BrCH_2CH_2NH_2$-HBr

Because of the importance of bromoethylamine in chemical modification rescue, a protein CRABPII-CLE that replaced the lysine residue with a cysteine was prepared following previously reported protocols. Both mutants, CRABPII-CLE and the alkylated mutant, were investigated for protonated Schiff base formation with retinal. The thiol group of the cysteine would be unable to form a PSB and, as expected, only an absorption peak around 370 nm was observed, due to free retinal (Fig. 3). The alkylation of the thiol in the cysteine with bromoethylamine would result in the formation of thiolysine (Fig. 1). The thiolysine formed contained a nucleophilic amine that would lead to Schiff base formation when reacted with retinal. Indeed, a bathochromic shift was observed to around 457 nm, indicative of PSB, suggesting that successful alkylation has been achieved.

Theoretical calculations

The attacking species (nucleophile) was considered to be HBr (Scheme 2), and protonation of the OH group was thought to take place prior to the nucleophilic attack as the reaction was run in excess acid. We did not consider an intramolecular attack, i.e., formation of the aziridinium ion, as in acidic conditions the amino functionality would be protonated, NH_3^+, hence it would not have the ability to act as a nucleophile. The gas phase calculated geometries of the relevant structures are summarized in Fig. 4. All reactant complex conformers present strong hydrogen bonds between the HBr and either protonated amino or hydroxyl groups, with the latter stronger by 31.4 kJ mol^{-1} (Table 3), due to presumably stronger acidity of the protonated hydroxyl group. This large difference could be attributed to the

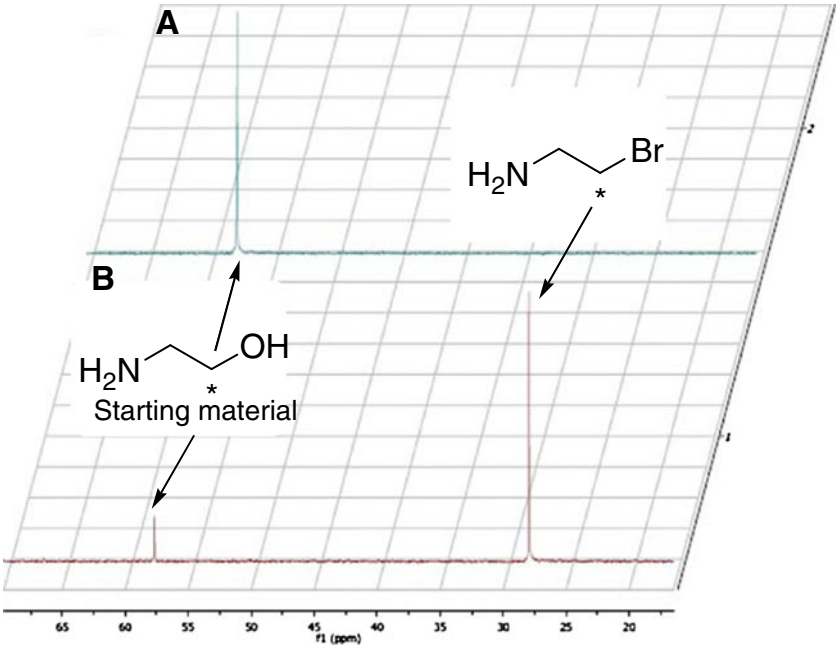

Fig. 2 ^{13}C NMR spectra of ethanolammonium bromide (**A**) and bromoethylamine (**B**)

electrostatic component that would manifest in gas-phase calculations, evidenced by the decrease of the gap between the two complexes to 8.0 kJ mol^{-1} when water was included in the model as solvent. Stabilization provided by the hydrogen bond does not seems to be affected by the relative position of the two groups, hydroxyl and amino, gauche or anti. Attack at the reaction site was modeled in a S_N2 manner and we considered backside attack guided by the interaction between the nucleophile (HBr) and the assisting group: $-NH_3^+$ (for attack at the CH_2-OH_2^+, Fig. 4, I) or -

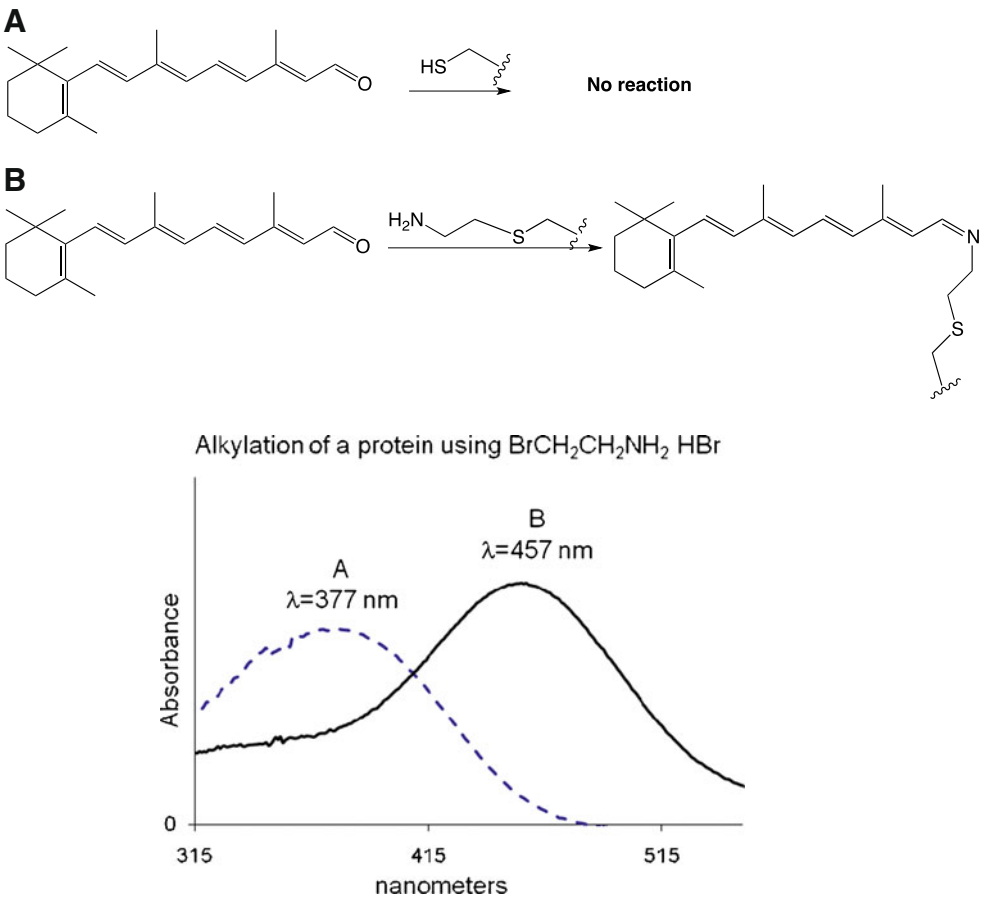

Fig. 3 UV–VIS spectra of retinal with unalkylated (**A**) and with alkylated protein (**B**)

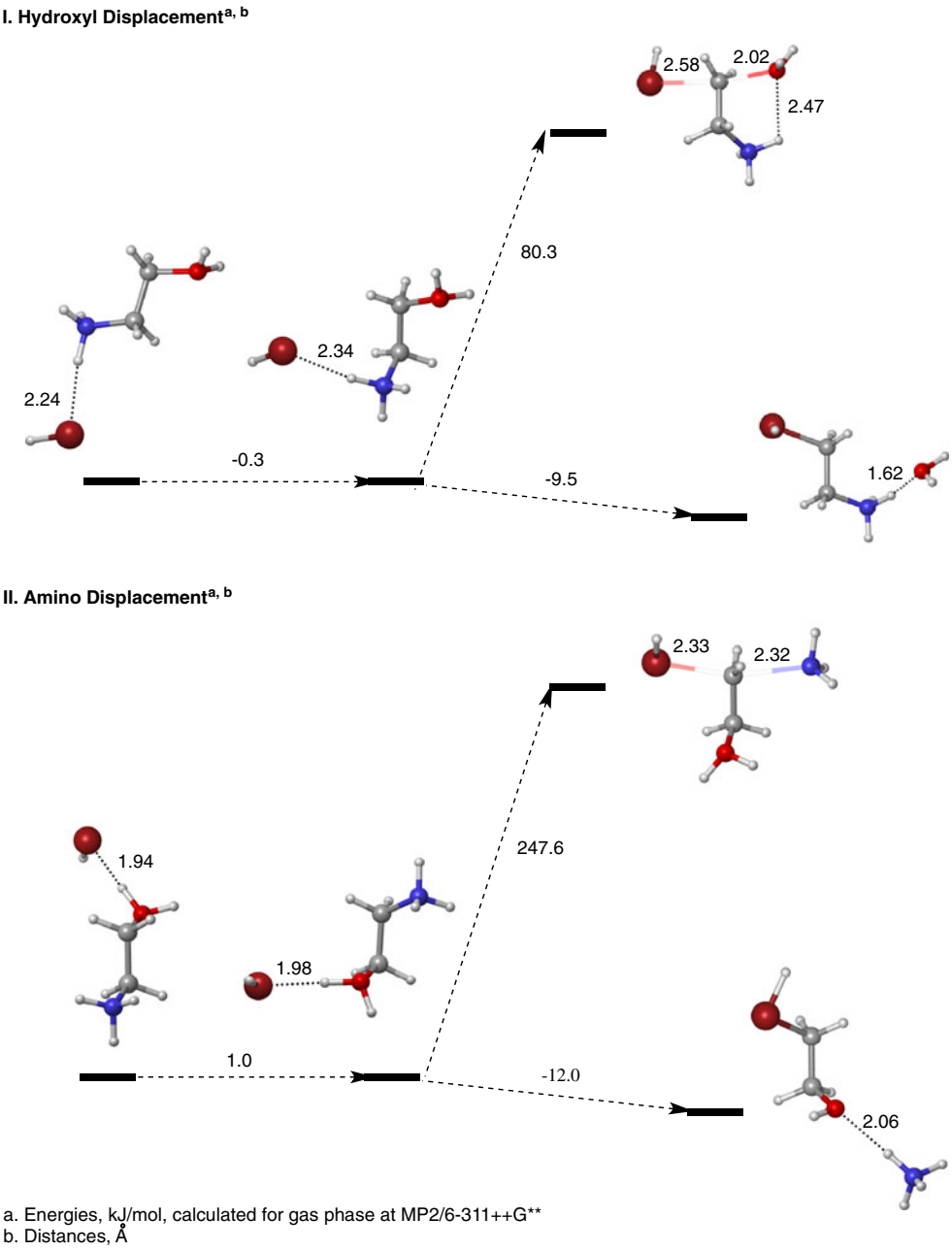

Fig. 4 Bromination of ethanolamine: reactant complexes, transition states, and products

Table 3 Energetics of bromination of ethanolamine

Starting complex	Conformer[a]	Association energy[b, c]	Activation barrier[b, c]	Overall energy[b, c]
$HBr\ldots NH_3CH_2CH_2OH_2$	gauche	54.4 (7.1)	80.3 (109.6)	−9.6
	anti	54.0 (6.3)	78.2 (98.7)	−10.9
$HBr\ldots OH_2CH_2CH_2NH_3$	gauche	85.4 (21.3)	247.7 (264.4)	−12.1
	anti	86.6 (15.9)	247.3 (253.1)	−12.1

[a] Conformers are defined with respect to the amino and hydroxyl relative positions

[b] Energies are corrected with ZPVE and expressed in kJ mol^{-1}

[c] First values are for gas-phase calculations, while values in parenthesis correspond to the solution reactions, at MP2/6-311++G**

Table 4 Energetics of alkylation of bromoethylamine

Nucleophile	Association energy[a, b]	Activation barrier[a, b]	Overall energy[a, b]
CH_3SH	26.4 (19.2)	186.6 (128.4)	−41.8 (−112.1)
CH_3S^-	63.2 (18.8)	33.9 (64.9)	−157.7 (−164.4)
NH_2	-	198.3 (105.0)	

[a] Energies are corrected with ZPVE and expressed in kJ mol^{-1}

[b] First values are for gas-phase calculations, while values in parenthesis correspond to the solution reactions, at MP2/6-311++G**

OH_2^+ (for attack at the CH_2-NH_3^+, Fig. 4, II). The transition states present the characteristics of classic S_N2 transition states, with the leaving group and the incoming nucleophile in a linear arrangement indicative of an sp^2 hybridized-like geometry around the C. One major difference would be in the proximity of the nucleophile; Br was closer to the C by 0.25 Å when the leaving group was NH_3^+. At the same time, the transition state corresponding to the hydroxyl displacement shows a weak hydrogen bond at 2.47 Å between the leaving group, H_2O, and NH_3. The barrier for the reaction that would lead to BEA, i.e., no scrambling, was found to be 80.3 kJ mol^{-1}, Table 3, lower by 167.4 kJ mol^{-1} compared to the pathway that would result in formation of bromoethanol. It is worth mentioning that the values obtained are similar to the calculations reported at a higher level of theory for similar substrates [52]. The attack at the OH_2^+-bearing side is favored by the better leaving group, H_2O versus NH_3 [53]. Interestingly, in both cases, at the transition state there is gauche interaction between the OH_2 and the NH_3 group regardless of the starting initial conformer,

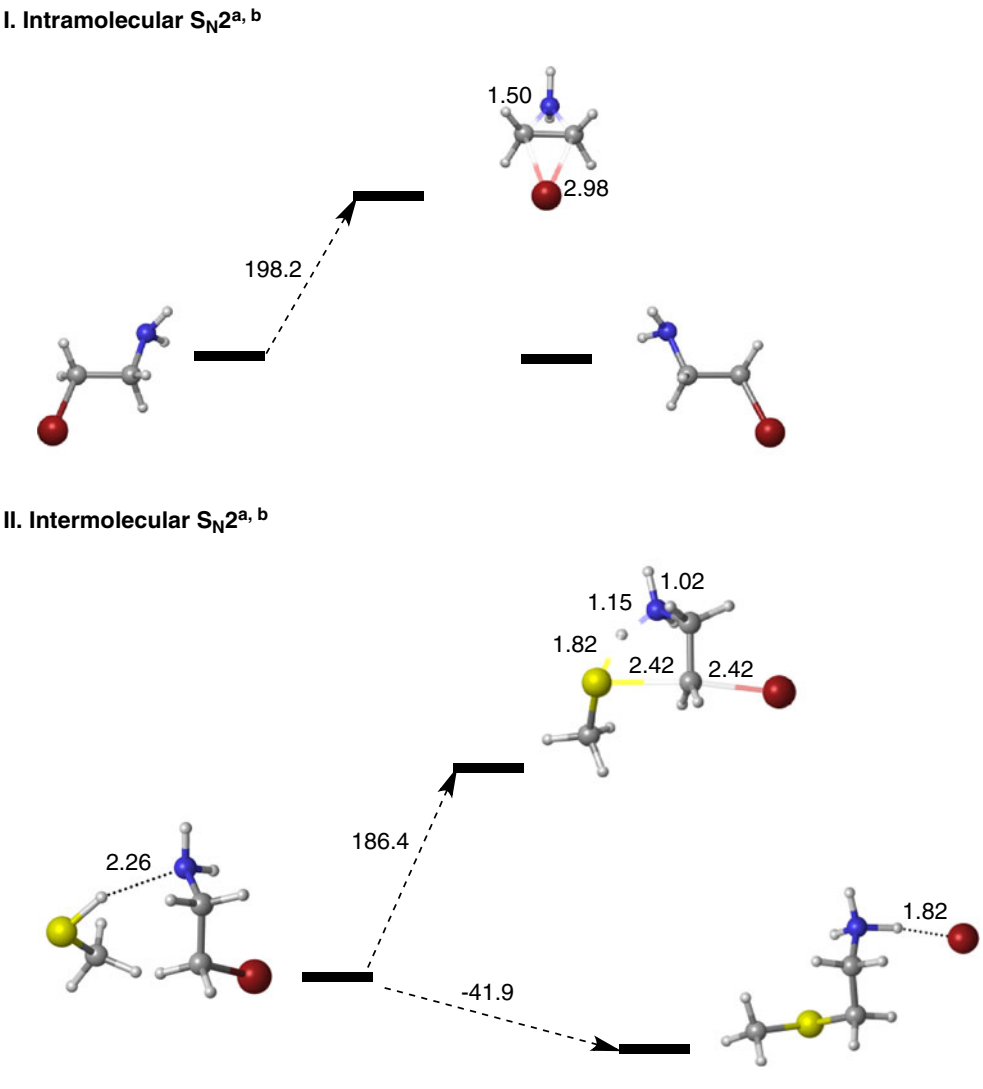

Fig. 5 Alkylation reaction: reactant complexes, transition states, and products

anti or gauche, and we interpret this to mean that assistance provided by the hydrogen bond takes place between HBr and OH_2^+ or NH_3^+ groups and later the interaction between the leaving group, H_2O and NH_3^+. These guiding hydrogen bonds induce rotation around the C–C bond.

For the alkylation reaction (Scheme 3), we considered that the model compound for the cysteine residue was CH_3SH. The alkylation reaction was run at basic pH=8.5 and thus the nature of the nucleophile comes into question: CH_3S^- or CH_3SH (if the environment around the cysteine residue is hydrophobic). Thus, as mentioned earlier, several pathways could be considered: intermolecular attack of either sulfur bearing nucleophile (CH_3SH or CH_3S^-) or intramolecular attack of the amino group. The results are summarized in Table 4.

Let us begin with a discussion of the gas phase results. The barrier for intramolecular substitution, i.e., formation of the aziridinium ring, is 198.3 kJ mol^{-1} (Fig. 5, I). Computational calculations (IRC) showed that the aziridium ring is a transition state in the scrambling process, due to the close proximity of the bromide, which back attacks to reform the bromoethylamine. The corresponding barrier for attack of CH_3SH, Fig. 5, II, is lower by 11.7 kJ mol^{-1} suggesting that the intermolecular pathway would be favored over the intramolecular one. The transition state for the substitution with CH_3SH has the characteristics of an S_N2 reaction, with both leaving group (Br) and nucleophile (CH_3SH) in vicinity of the C atom that undergoes the substitution at 2.42 Å distance each. Proton abstraction from CH_3SH by the amino group takes place at the same time with the nucleophilic attack, presumably due to both basicity of the NH_2 and close proximity between the two groups involved. The barrier for attack by an ionic and thus stronger nucleophile, CH_3S^-, at 33.9 kJ mol^{-1} is a drastically lower than the barriers corresponding to the other pathways considered.

Inclusion of water as solvent via a CPCM model affects the pathways with respect to both energetics and geometry. Presence of a polar protic solvent should stabilize the species in which charge development takes place, and that is indeed what we found with our calculations. The reaction that involves CH_3S^- as a nucleophile is favored over all the alternatives due to the fact that it involves an ionic reactant. However, at the transition state the charge is less separated than in the reactants, leading to preferential stabilization of the reactants by the solvent and thus there is an increase in the activation barrier, from 33.9 kJ mol^{-1} (gas-phase) to 64.9 kJ mol^{-1} (solution). On the other hand the other two reactions involve neutral species and partial charge development takes place at the transition state, which should lead to a decrease in the activation barrier when compared to the gas-phase reaction, and indeed that is the case. However, CH_3SH is bulkier and the charge will be more diffuse at the transition state compared to the intramolecular case involving the amino group. As a result, the reduction of the activation barrier is more pronounced for the latter case, leading to values of 105.0 and 128.4 kJ mol^{-1} for NH_2 and CH_3SH, respectively. These findings suggest that, in presence of water at neutral pH, intramolecular substitution is favored over intermolecular attack by the CH_3SH, a reversed trend compared to gas phase. However at basic pH the sulfur nucleophile is deprotonated and thus the reaction barrier is the lowest for intermolecular attack by CH_3S^-.

Summary

We synthesized singly labeled bromoethylamine in acid conditions and we modeled the reaction at MP2/6-311++G** level in both gas phase and solution. Our results suggest that the nucleophilic attack takes place only at the C bearing the OH group and that hydrogen bonds play a role in guiding the attack. Application of this alkylating agent does show modification of the protein's UV spectrum, indicative of successful alkylation. Modeling of the alkylation reaction suggests that attack by the neutral thiol group is favored over intramolecular scrambling in gas phase (which would correspond to a hydrophobic environment). Solution modeling points in the direction of a lowest barrier for intermolecular attack by the thiolate, which would be the state of the sulfur-bearing nucleophile in aqueous solution at the reaction pH.

References

1. Vitzthum F, Behrens F, Anderson L, Shaw JH (2005) Proteomics: from basic research to diagnostic application. A review of requirements and needs. J Proteome Res 4:1086–1097
2. Gloerich J, Wevers RA, Smeitink JAM, van Engelen BG, van den Heuvel LP (2007) Proteomics approaches to study metabolic and genetic disorders. J Proteome Res 6:506–512
3. Sakal AGE, Shechter Y (1991) Biological activity of a fluorescein human growth hormone derivative prepared by specific covalent labeling of lysine-70. Biochemistry 30:8899–8904
4. Aison SP, Hindley D, Wang L, Shah K, Wang Y, Hu X, Shokar KM, Kolch W, Sedivy JM, Yeung KC (2004) Engineering the serine/threonine protein kinase Raf-1 to utilize an orthogonal analogue of ATP substituted at the N^6 position. FEBS Lett 556:26–34
5. Hermanson GT (1996) Bioconjugate techniques, 1st edn. Academic, New York
6. Giron P, Dayon L, Sanchez JC (2011) Cysteine tagging for MS-based proteomics. Mass Spectrom Rev 30:366–395
7. Brotzel F, Mayr H (2007) Nucleophilicities of amino acids and peptides. Org Biomol Chem 5:3814–3820
8. Gregori L, Poosch MS, Cousins G, Chaw V (1990) A uniform isopeptide-linked multiubiquitin chain is sufficient to target substrate for degradation in ubiquitin-mediated proteolysis. J Biol Chem 265:8354–8357
9. Raftery MA, Cole D (1996) On the aminoethylation of proteins. J Biol Chem 241:3457–3459
10. Piotrowski J, Beal R, Hoffman L, Wilkinson KD, Cohen RE, Pickart CM (1997) Inhibition of the 26 S Proteasome by

polyubiquitin chains synthesized to have defined lengths. J Biol Chem 272:23712–23721
11. Gorlatov SN, Stadtman TC (1998) Human thioredoxin reductase from HeLa cells: Selective alkylation of selenocysteine in the protein inhibits enzyme activity and reduction with NADPH influences affinity to heparin. Proc Natl Acad Sci USA 95:8520–8525
12. Hartmann S, Hofsteenge J (2000) Protein synthesis post-translation modification and degradation. J Biol Chem 275:28569–28574
13. Hopkins CE, O'Connor PB, Allen KN, Costello CE, Tolan DR (2002) Chemical-modification rescue assessed by mass spectrometry demonstrates that γ-thia-lysine yields the same activity as lysine in aldolase. Protein Sci 11:1591–1599
14. Jacobson MSG, Stark G, Vanaman T (1973) Specific chemical cleavage in high yield at the amino peptide bonds of cysteine and cysteine residues. J Biol Chem 248:6583–6591
15. Robert TKH, Czerwinski M, Johnson WH Jr, Legler PM, Tivers JT, Mildvan AS, Whitman CP (1999) Effects of mutations of the active site arginine residues in 4-oxalocrotonate tautomerase on the pK_a values of active site residues and on the pH dependence of catalysis. Biochemistry 38:12358–12366
16. Garrod EHS, Connor SC, Connely JC, Spraul M, Nicholson JC, Holmes E (2001) High-resolution ^{1}H NMR and magic angle spinning NMR spectroscopic investigation of the biochemical effects of 2-bromoethanamine in intact renal and hepatic tissue. Magn Res Med 45:781–790
17. Hopkins CE, Hernandez G, Lee JP, Tolan DR (2005) Aminoethylation in model peptides reveals conditions for maximizing thiol specificity. Arch Biochem Biophys 443:1–10
18. Thevis M, Ogorzalek Loo RR, Loo JA (2003) In-gel derivatization of proteins for cysteine-specific cleavages and their analysis by mass spectrometry. J Proteom Res 2:163–172
19. Řehulková H, Marchetti-Deschmann M, Pittenauer E, Allmaier G, Řehulka P (2009) Improved identification of hordeins by cysteine alkylation with 2-bromoethylamine, SDS-PAGE and subsequent in-gel tryptic digestion. J Mass Spectrom 44:1613–1621
20. Wystrach VP, Kaiser DW, Schaefer FC (1955) Mono-(1-aziridinyl)-s-triazines and bis-(1-aziridinyl)-s- triazines. J Am Chem Soc 77:5918–5922
21. Bach PL, Bridges J (1982) Synthesis of 2-bromo-1-^{14}C]ethanamine hydrobromide. J Label Compd Radiopharm 19:425–431
22. Bird I, Farmer PB (1988) The synthesis of deuterium-labelled 2-bromoethanol, acrylonitrile, acrylamide, 2-aminoethanol, 2-bromethylamine hydrobromide and 1-bromo-2-chloroethane. J Label Compd Radiopharm 27:199–216
23. Schutte E, Weakle RJR, Tyler DR (2003) Radical cage effects in the photochemical degradation of polymers: effect of radical size and mass on the cage recombination efficiency of radical cage pairs generated photochemically from the (CpCH2CH2N(CH3)C(O)(CH2)nCH3)2Mo2(CO)6 (n = 3, 8, 18) complexes. J Am Chem Soc 125:10319–10326
24. Nagle AS, Salvatore RN, Byong-Don C, Jung KW (2000) Efficient synthesis of β-amino bromides. Tetrahedron Lett 41:3011–3014
25. Vasileiou C, Vaezeslami S, Crist RM, Rabago-Smith M, Geiger JH, Borhan B (2007) Protein design: Reengineering cellular retinoic acid binding protein II into a Rhodopsin protein mimic. J Am Chem Soc 129:6140–6148
26. Frisch MJ, Trucks GW, Schlegel HB, Scuseria GE, Robb MA, Cheeseman JR, Scalmani G, Barone V, Mennucci B, Petersson GA, Nakatsuji H, Caricato M, Li X, Hratchian HP, Izmaylov AF, Bloino J, Zheng G, Sonnenberg JL, Hada M, Ehara M, Toyota K, Fukuda R, Hasegawa J, Ishida M, Nakajima T, Honda Y, Kitao O, Nakai H, Vreven T, Montgomery JA Jr, Peralta JE, Ogliaro F, Bearpark M, Heyd JJ, Brothers E, Kudin KN, Staroverov VN, Kobayashi R, Normand J, Raghavachari K, Rendell A, Burant JC, Iyengar SS, Tomasi J, Cossi M, Rega N, Millam NJ, Klene M, Knox JE, Cross JB, Bakken V, Adamo C, Jaramillo J, Gomperts R, Stratmann RE, Yazyev O, Austin AJ, Cammi R, Pomelli C, Ochterski JW, Martin RL, Morokuma K, Zakrzewski VG, Voth GA, Salvador P, Dannenberg JJ, Dapprich S, Daniels AD, Farkas Ö, Foresman JB, Ortiz JV, Cioslowski J, Fox DJ (2009) Gaussian 09, Revision B.01. Gaussian, Wallingford
27. Head-Gordon M, Pople JA, Frisch MJ (1988) MP2 energy evaluation by direct methods. Chem Phys Lett 153:503–506
28. Francl MM, Pietro WJ, Hehre WJ, Binkley JS, Gordon MS, Defrees DJ, Pople JA (1982) Self-consistent molecular orbital methods. 23. A polarization-type basis set for 2nd-row elements. J Chem Phys 77:3654–3665
29. Lee CT, Yang WT, Parr RG (1988) Development of the Colle-Salvetti correlation-energy formula into a functional of the electron density. Phys Rev B 37:785–789
30. Becke ADJ (1993) Density-functional thermochemistry. III. The role of exact exchange. J Chem Phys 98:5648–5652
31. Hoe W-M, Cohen A, Handy NC (2001) Assessment of a new local exchange functional OPTX. Chem Phys Lett 341:319–328
32. Raghavachari K, Binkley JS, Seeger R, Pople JA (1980) Self-consistent molecular orbital methods. 20. Basis set for correlated wave-functions. J Chem Phys 76:650–654
33. McLean AD, Chandler GS (1980) Contracted Gaussian-basis sets for molecular calculations. 1. 2nd row atoms, Z=11-18. J Chem Phys 72:5639–5648
34. Clark T, Chandrasekhar GW, Spitznagel GW, PvR S (1983) Efficient diffuse function-augmented basis-sets for anion calculations. 3. The 3-21+G basis set for 1st-row elements, Li-F. J Comput Chem 4:294–301
35. Frisch MJ, Pople JA, Binkley JS (1984) Self-consistent molecular orbital methods. 25. Supplementary functions for Gaussian basis sets. J Chem Phys 80:3265–3269
36. Baker J, Pulay P (2002) Assessment of the Handy-Cohen optimized exchange density functional for organic reactions. J Chem Phys 117:1441–1449
37. Xu X, Goddart WA III (2004) Assessment of Handy−Cohen Optimized Exchange Density Functional (OPTX). J Phys Chem A 108:8495–8504
38. Gung VA, Khuong KS, Houk KN, Chuma A, Pulay P (2004) The Performance of the Handy/Cohen functionals, OLYP and O3LYP, for the computation of hydrocarbon pericyclic reaction activation barriers. J Phys Chem A 108:2959–2965
39. Gonzales JM, Allen WD, Schaeffer HF III (2005) Model identity S_N2 reactions $CH_3X + X^-$ (X = F, Cl, CN, OH, SH, NH_2, PH_2): Marcus theory analyzed. J Phys Chem A 109:10613–10628
40. Bento AP, Sola M, Bickelhaupt FM (2005) Ab initio and DFT benchmark study for nucleophilic substitution at carbon (S(N)2@C) and Silicon (S(N)2@Si). J Comput Chem 26:1497–1504
41. Swart M, Sola M, Bickelhaupt FM (2007) Energy landscapes of nucleophilic substitution reactions: a comparison of density functional theory and coupled cluster methods. J Comput Chem 28:1551–1560
42. Zhao Y, Truhlar DG (2008) Density functionals with broad applicability in chemistry. Acc Chem Res 41:157–167
43. Bento AP, Sola M, Bickelhaupt FM (2008) E2 and S(N)2 reactions of X- + CH3CH2X (X = F, Cl); an ab initio and DFT benchmark study. J Chem Theor Comput Chem 4:929–940
44. Baker J, Muir M, Anzelm J (1995) A study of some organic reactions using density functional theory. J Chem Phys 102:2063–2080
45. Barone V, Adamo C (1996) Proton transfer in the ground and lowest excited states of malonaldehyde: a comparative density functional and post–Hartree–Fock study. J Chem Phys 105:11007–11020
46. Bach RD, Glukhotsev MN, Gonzales C (1998) High-level computational study of the stereoelectronic effects of substituents on alkene epoxidations with peroxyformic acid. J Am Chem Soc 120:9902–9910
47. Gritsenko OV, Ensing B, Schippers PRT, Baerends EJ (2000) Comparison of the accurate Kohn−Sham solution with the

generalized gradient approximations (GGAs) for the SN2 Reaction F- + CH3F → FCH3 + F-: a qualitative rule to predict success or failure of GGAs. J Phys Chem A 104:8558–8565
48. Krenske EH, Peter RC, Zhu Z, Houk KN (2011) Transition States and Energetics of nucleophilic additions of thiols to substituted α, β-unsaturated ketones: substituent effects involve enone stabilization, product branching, and solvation. J Org Chem 76:5074–5081
49. Barone V, Cossi M (1998) Quantum calculation of molecular energies and energy gradients in solution by a conductor solvent model. J Phys Chem A 102:1995–2001
50. Cossi M, Rega N, Scalmani G, Barone V (2003) Energies, structures, and electronic properties of molecules in solution with the C-PCM solvation model. J Comput Chem 24:669–681
51. Legault CY (2009) CYLview, 1.0b, Université de Sherbrooke. (http://www.cylview.org)
52. Laerdahl JK, Uggerud E (2003) Part I. Nucleophilic identity substitution reactions. The reaction between water and protonated alcohols. Org Biomol Chem 1:2935–2942
53. Jaramillo P, Domingo LR, Perez P (2006) Towards an intrinsic nucleofugality scale: the leaving group (LG) ability in CH(3)LG model system. Chem Phys Lett 420:95–99